PAPER

Visible emission spectra of thermographic phosphors under x-ray excitation

To cite this article: Eric R Westphal *et al* 2021 *Meas. Sci. Technol.* **32** 094008
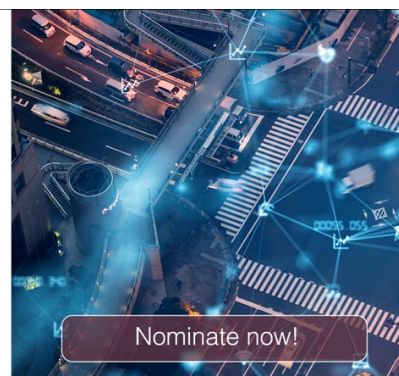
View the article online for updates and enhancements.

Visible emission spectra of thermographic phosphors under x-ray excitation

Eric R Westphal[1],*, **Alex D Brown**[1], **Enrico C Quintana**[2], **Alan L Kastengren**[3], **Steven F Son**[1], **Terrence R Meyer**[1] and **Kathryn N G Hoffmeister**[2],*

[1] School of Mechanical Engineering, Purdue University, West Lafayette, IN 47907, United States of America
[2] Sandia National Laboratories, Albuquerque, NM 87123, United States of America
[3] X-ray Science Division, Advanced Photon Source, Argonne National Laboratory, Argonne, IL 60439, United States of America

E-mail: ewestph@purdue.edu and kngabet@sandia.gov

CrossMark

Abstract

Thermographic phosphors have been employed for temperature sensing in challenging environments, such as on surfaces or within solid samples exposed to dynamic heating, because of the high temporal and spatial resolution that can be achieved using this approach. Typically, UV light sources are employed to induce temperature-sensitive spectral responses from the phosphors. However, it would be beneficial to explore x-rays as an alternate excitation source to facilitate simultaneous x-ray imaging of material deformation and temperature of heated samples and to reduce UV absorption within solid samples being investigated. The phosphors $BaMgAl_{10}O_{17}$:Eu (BAM), Y_2SiO_5:Ce, YAG:Dy, La_2O_2S:Eu, $ZnGa_2O_4$:Mn, $Mg_3F_2GeO_4$:Mn, Gd_2O_2S:Tb, and ZnO were excited in this study using incident synchrotron x-ray radiation. These materials were chosen to include conventional thermographic phosphors as well as x-ray scintillators (with crossover between these two categories). X-ray-induced thermographic behavior was explored through the measurement of visible spectral response with varying temperature. The incident x-rays were observed to excite the same electronic energy level transitions in these phosphors as UV excitation. Similar shifts in the spectral response of BAM, Y_2SiO_5:Ce, YAG:Dy, La_2O_2S:Eu, $ZnGa_2O_4$:Mn, $Mg_3F_2GeO_4$:Mn, and Gd_2O_2S:Tb were observed when compared to their response to UV excitation found in literature. Some phosphors were observed to thermally quench in the temperature ranges tested here, while the response from others did not rise above background noise levels. This may be attributed to the increased probability of non-radiative energy release from these phosphors due to the high energy of the incident x-rays. These results indicate that x-rays can serve as a viable excitation source for phosphor thermometry.

Keywords: thermographic phosphors, x-ray scintillation, temperature sensing

(Some figures may appear in colour only in the online journal)

---

* Authors to whom any correspondence should be addressed.

1. Introduction

As an important state variable, considerable effort is often made to accurately measure the temperature of surfaces or within solid samples exposed to dynamic heating and/or reacting environments. Knowledge of material temperature is required to accurately predict heat transfer to surfaces exposed to gas-phase reactions or to interfaces/features within solid samples undergoing frictional or strain-induced heating. This in turn provides information on the ignition and burning-rate characteristics of the reacting material. Such information is often desired when characterizing hotspot formation [1] or combustion behavior of solid propellants [2, 3]. Conventional methods of material temperature measurement include embedded thermocouples and pyrometry. Both methods can be useful in certain applications but have intrinsic drawbacks. Thermocouples only provide a single point measurement of temperature and can suffer from thermal lag, yielding poor spatial and temporal resolution. Errors can also be introduced using thermocouples from catalytic effects in the measurement medium [4], as well as uncertainties due to radiative heat transfer [5]. Pyrometry has the potential to provide surface temperature measurements in more than one spatial dimension, however, the emissivity of the measured surface is needed for determining temperature from the measured emission and can introduce significant uncertainties [6]. A method which can potentially overcome the drawbacks of these other methods is phosphor thermometry, which is the focus of the present study. In this technique, thermographic phosphor particles are excited by a light source and undergo electronic energy level transitions to levels above their ground state. Once excitation is ceased, these particles follow an energy cascade down to their ground state, during which energy is released both radiatively and non-radiatively. The non-radiative energy release from the phosphors varies with temperature, leading to concommitant shifts in their radiative spectral properties.

It is possible to obtain information about spatial distributions and temporal variations of temperature through the appropriate selection of phosphor and method for extracting temperature information from their induced emission. Two primary methods exist, one in which the emission decay is measured in time (lifetime method), and the other in which two different spectral bands of the emission are measured and used to obtain a temperature dependent, calibrated intensity ratio (ratio method). The lifetime decay of thermographic phosphor emission typically decreases with increasing temperature and ranges from hundreds of microseconds to nanoseconds, making temperature measurements at these time resolutions possible with appropriate phosphor selection [7, 8]. In addition, using the ratio of spectral bands allows for temperature measurements ranging from room temperature up to 1700 K [9] and has successfully enabled temperatures to be measured in two dimensions using high-speed cameras [10–12].

The typical source for excitation of thermographic phosphors is a laser emitting in the UV or visible range [7]. Light emitting diodes emitting in this range have also been employed for phosphor excitation [13–16]. In certain applications, however, it may be beneficial to explore the use of x-rays as an alternate source for excitation of thermographic phosphors. These include situations in which x-rays can be used for simultaneous investigation of the structural and thermal response of a reacting material when exposed to transient heating phenomena (e.g. burning solid propellants and reacting energetic crystals). When excited via x-rays, the visible response from phosphors is a form of x-ray excited optical luminescence (XEOL). As incident x-rays can more easily penetrate solid materials and reach embedded phosphors, this technique would also be useful in applications in which dynamic structural properties may perturb the passage of UV photons, such as soot in the gas phase of flames. In each of these cases, excitation of thermographic phosphors using x-rays could simplify the experimental setup and/or interpretation of recorded signals for more accurate temperature measurements.

To this end, several thermographic phosphors were excited by synchrotron x-ray radiation in this study, and their spectral response was characterized over a range of temperatures. Phosphors were selected, in part, based upon the usefulness of their known emission spectra when excited via a laser for combustion applications. Some of the phosphors selected are also known scintillators, in addition to having a thermographic response when excited by UV radiation. Previous work from the authors has shown that the XEOL from one such phosphor, Gd_2O_2S:Tb, remains thermographic when excited by an x-ray tube source [17]. Other studies have shown the ability to measure XEOL signal from the phosphors La_2O_2S:Eu [18] and Gd_2O_2S:Eu [19] through tissue. Though each of these phosphors are thermographic, temperature sensing was not the focus of either study. However, their results support the hypothesis that a temperature sensitive XEOL response would allow for temperature sensing in environments not suitable for or more challenging for conventional laser excitation of phosphors. This work represents a comprehensive study of the temperature sensitivity of numerous phosphors under x-ray excitation for the first time.

2. Background

Thermographic phosphors are typically composed of a ceramic host matrix along with impurities introduced via doping. These impurities are either rare-earth or transition metal ions and are commonly referred to as activators since luminescence originates from these dopants [7]. Emission from phosphors results from the radiative energy transfer these materials experience as they relax to their ground state from an excited state. Non-radiative energy transfer also occurs (such as through phonon emission), causing the emitted light to be red-shifted from the excitation source (i.e. Stokes-shifted). Competing effects of the radiative and non-radiative energy release cause the temperature dependence seen in thermographic phosphors.

The scintillation process of phosphors under x-ray excitation first starts with penetration of the phosphor crystal lattice by the incident x-rays. Ionization of atoms within the crystal occurs, ejecting an electron from an inner shell (typically the K shell) of each atom [20]. These vacancies are then

filled, producing either characteristic x-rays (radiative energy release) or Auger electrons (non-radiative energy release). The former of these two can be reabsorbed at a different location in the crystal lattice, causing further ionization. This ionization will move from K to L or M shells as relaxation occurs and photon energy is reduced [20]. The ejected primary or Auger electrons dissipate energy through scattering electrons or phonon emission [20]. This form of energy cascade occurs until the energy release from the atoms cannot produce further ionization.

During excitation and subsequent relaxation of the phosphor crystals, electronic excitations of the crystal structure can transfer their energy to the activators [20]. These activators introduce luminescence and quenching centers in the crystal structure through the addition of local energy levels corresponding to the ground and excited states of these centers [21]. Excitation of one of these centers requires the center to capture an electron in the conduction band and a hole in the valence band of the phosphor, either consecutively through electron–hole recombination or simultaneously through the capture of an exciton [20, 21]. The radiative and non-radiative energy release experienced by these centers after excitation are responsible for the photon and phonon emission typically seen during phosphor thermometry, respectively. See Khalid and Kontis for a succinct description of how a ceramic host matrix and a rare-earth activator can interact to produce thermographic emission [22]. The photoemission originating from the luminescence centers described here are the focus of the present study.

The energy gap between the excited and ground states of these centers correspond to emission typically in the visible region and can therefore be imaged using conventional methods, such as using a photomultiplier tube, photodiode, or high-speed camera. The method by which emission is captured is dictated by the spectral properties to be analyzed for their temperature dependence. Two primary methods exist for phosphor thermometry, the first being the measurement of lifetime decay of the phosphor emission. This lifetime decay is typically modeled to follow a simple mono-exponential decay of the following form:

$$I(t) = I_0 * \exp\left(-\frac{t}{\tau}\right) + b$$

where I_0 is the initial intensity of the decay, t is time, τ is the time constant, and b is the background offset intensity (i.e. noise floor). Numerical methods are typically employed for calculating the temperature dependent time constant, such as a Levenburg–Marquardt algorithm [23]. The lifetime of thermographic phosphors can range from milliseconds to nanoseconds [8]; therefore, phosphor selection is often influenced by the expected lifetime. Single-point temperature measurements are often made using the lifetime method as it can be difficult or costly to employ two-dimensional detectors that can capture emission at rates high enough to fully resolve the decay. In general, the detector used to capture emission should operate at orders of magnitude faster than the repetition rate of the excitation source to fully resolve the lifetime decay.

The second method of phosphor thermometry involves taking the ratio of two spectral bands of the emission to create a temperature dependent intensity ratio calibration curve. Shifts in energy level populations described previously lead to variations in emission intensity strength of some spectral lines of select phosphors, leading to this type of temperature sensitivity. Broadening can also be seen in spectral lines at elevated temperatures due to the increased populations of various vibrational states in the excited electronic state. This increases the probability of radiative transitions between more of these vibrational levels in the excited and ground electronic states [22]. The ratio is typically taken instead of measuring single spectral line intensities to reduce errors introduced by variations in absolute intensity between experiments and setups [8, 24, 25]. Emission can be captured using a spectrometer or by optically filtering the emission sent to two different detectors. This method is more commonly used at high sample rates and to measure two-dimensional temperature fields since the lifetime decay no longer needs to be resolved.

The visible emission from phosphors excited via x-rays is commonly used for x-ray detection (in which the phosphors are known as x-ray scintillators) [26]. For example, scintillators are used in medical x-ray imaging to reduce patient exposure to x-rays through the production of many UV or visible photons from a single incident x-ray photon [27]. The phosphor Gd_2O_2S:Tb is one such x-ray scintillator, though this phosphor is also known to produce a thermographic response under UV excitation [28]. This phosphor, along with other x-ray scintillators and several conventional thermographic phosphors, were evaluated in this study for a thermographic response in their spectral response under x-ray excitation.

3. Experimental methods

Most of the phosphors selected for this study were obtained from Phosphor Technology Ltd (PTL). These included $BaMgAl_{10}O_{17}$:Eu or BAM (PTL KEMK63), Y_2SiO_5:Ce (PTL QBK58), YAG:Dy (PTL QMK66), La_2O_2S:Eu (PTL SKL63), $ZnGa_2O_4$:Mn (PTL GPK25), Gd_2O_2S:Tb (PTL UKL65), $Mg_3F_2GeO_4$:Mn (PTL EQD25), and ZnO (Just Pigments, ZN001-1). These are all known to produce a thermographic response from laser excitation [8, 29, 30]. In addition, the phosphors Gd_2O_2S:Tb [27], La_2O_2S:Eu [31], and Y_2SiO_5:Ce [20] are commonly used as scintillators and are therefore expected to produce a visible response when excited via x-rays.

Samples were prepared by first mixing each phosphor powder with a small amount of ethanol. This mixture was applied to the surface of an aluminum substrate using a brush, and the ethanol was allowed to evaporate. Samples were then placed on a hot plate along with a blank Al substrate, the latter of which was used to collect background spectra for later background subtraction of each phosphor emission spectrum. This setup was placed in the beam path of beamline 7-BM-B at the Advanced Photon Source at Argonne National Laboratory. This beamline was set to monochromatic beam mode during testing and produced x-rays with energies of 67.6 keV
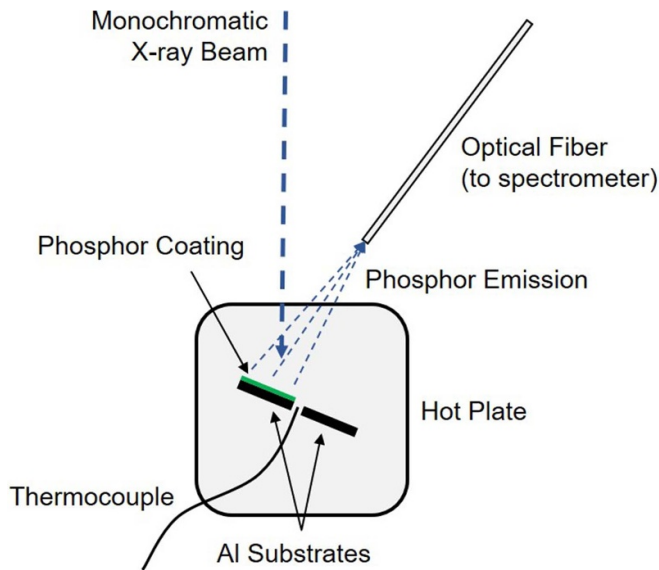
Figure 1. Schematic of the experimental setup used at the Advanced Photon Source.

with a 1% bandpass. The beam spot size which illuminated each sample was set to a square with sides of length 0.2 mm. Attenuation of the x-ray beam was achieved using combinations of Si, Cu, and Ge filters. This was performed to adjust incident radiation intensity to balance spectrometer integration time and signal to noise ratio for each sample. Filter combinations were kept consistent for each phosphor between each temperature tested.

During testing, temperature of the sample was adjusted by varying the hot plate temperature. A thermocouple was placed on the surface of the hot plate in between (and in contact with) the blank and coated Al substrates to monitor temperature. Emission spectra from the phosphor samples were captured using focusing optics (plano-convex lenses, Thorlabs) and an optical fiber (Ocean Optics QBIF600-UV-VIS). This optical fiber was routed to the input of an Ocean Optics OCEAN-FX-XR1-ES spectrometer for characterization. Figure 1 shows a schematic of the experimental setup. A total of 50 emission spectra were captured from each phosphor at each temperature tested along with ten background spectra. These were later averaged, and each average phosphor signal spectrum was background subtracted using the corresponding average background spectrum.

4. Results

4.1. $BaMgAl_{10}O_{17}$:Eu (BAM)

The induced emission of BAM originates from the $4f^65d \rightarrow 4f^7$ transition of its Eu^{2+} activator [32]. Influences of the host material on the Eu^{2+} activator ions lead to a broad emission band centered near 440 nm. Specifically, Stark splitting of the $4f^65d$ level of Eu^{2+} due to the electric field of the host lattice dictates the wavelength of the spectral band [32].

Figure 2 shows the emission captured from this phosphor at two different temperatures. A larger number of temperature increments is ideal, though time constraints at the beamline
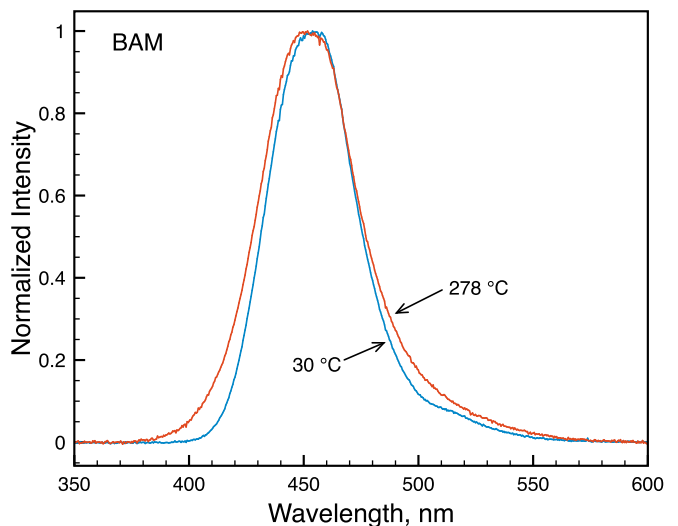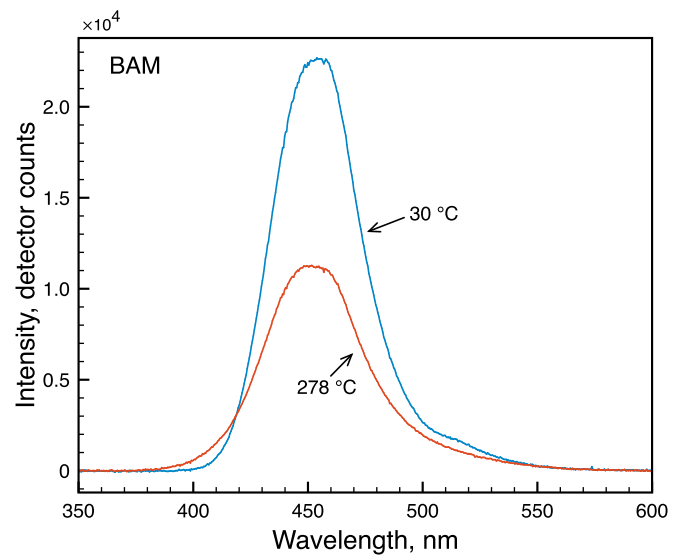

Figure 2. The non-normalized (top) and normalized (bottom) emission spectra of BAM at two different temperatures. The spectrometer integration time was set to 5 s when capturing these spectra.

limited the number of increments that could be tested for each phosphor. Both the absolute and normalized intensity are shown in this figure. Note that emission is attenuated with an increase in temperature. This is a common theme observed in the spectral response of all the phosphors tested and is expected due to the increased probabilities of non-radiative transitions of the activator ions back down to their ground state at elevated temperatures (i.e. thermal quenching). Broadening of this peak is observed with elevated temperature, which is also present in the emission of BAM induced by UV excitation [9].

4.2. Y_2SiO_5:Ce

The phosphor Y_2SiO_5:Ce is activated by Ce^{3+} and exhibits emission originating from the $5d^1 \rightarrow 4f^1$ transition of this ion [20, 32]. Shionoya and Yen note that emission from this ion has been observed to decay the fastest of the lanthanides since
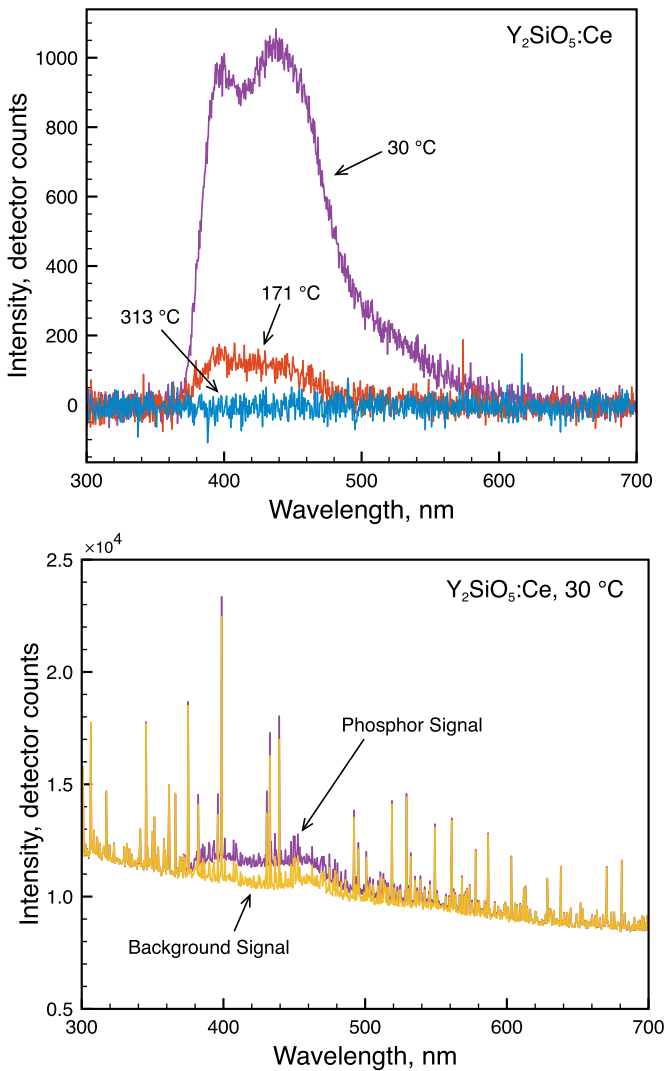
Figure 3. Top: The non-normalized emission spectra of Y_2SiO_5:Ce at various temperatures. Bottom: The phosphor emission spectrum (without background subtraction) and background spectrum captured at 30 °C, showing little rise in the emission from this phosphor above background levels. The spectrometer integration time was set to 5 s when capturing all of these spectra.

Figure 4. Top: The normalized emission spectra of YAG:Dy at various temperatures. The spectrometer integration time was set to 5 s when capturing these spectra. Bottom: The intensity ratio of two different spectral bands in these emission spectra at each temperature tested. The shaded areas in the top plot represent the bands used to find the ratio in bottom plot.

this d → f transition is both parity-allowed and spin-allowed, as these two states are spin doublets [32]. This has led to interest in using this phosphor in combustion applications. The top plot of figure 3 shows the emission spectra recorded for this phosphor under x-ray excitation at three different temperatures. Two overlapping peaks are present in the emission spectra centered near 420 nm, which matches the location of this phosphor's emission under UV laser excitation [9]. Note that this plot is given in absolute intensity (no normalization) and shows very low detector counts, indicating that emission did not rise substantially above background levels. This fact is highlighted in the bottom plot of figure 3, showing the largest emission intensity observed for this phosphor (at 30 °C, without background subtraction) relative to the averaged background emission spectrum. This indicates that this phosphor would most likely not be useful for thermometry
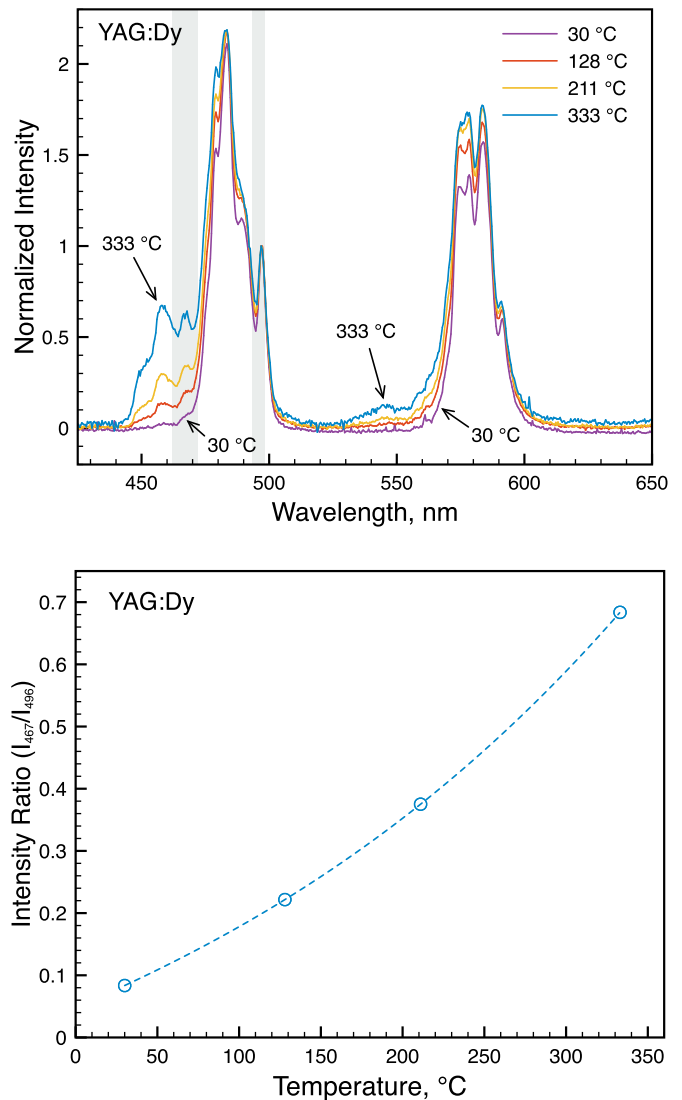
when using x-rays for excitation. Note that the various spikes that appear in both the background and phosphor signal in the bottom plot are from scattered background emission picked up by the spectrometer and are therefore not present in the top plot after background subtraction.

4.3. YAG:Dy

Dy^{3+} is another lanthanide commonly used as an activator in phosphors with various host materials. When doped into $Y_3Al_5O_{12}$ (YAG) it shows temperature sensitivity up to 1800 K [33]. The spectral response of YAG:Dy is expected to have bands originating from Dy^{3+} in the regions 470 nm to 500 nm and 570 nm to 600 nm, which correspond to the $^4F_{9/2} \rightarrow {}^6H_{15/2}$ and $^6F_{15/2} \rightarrow {}^6F_{11/2}$ transitions, respectively [32]. Figure 4
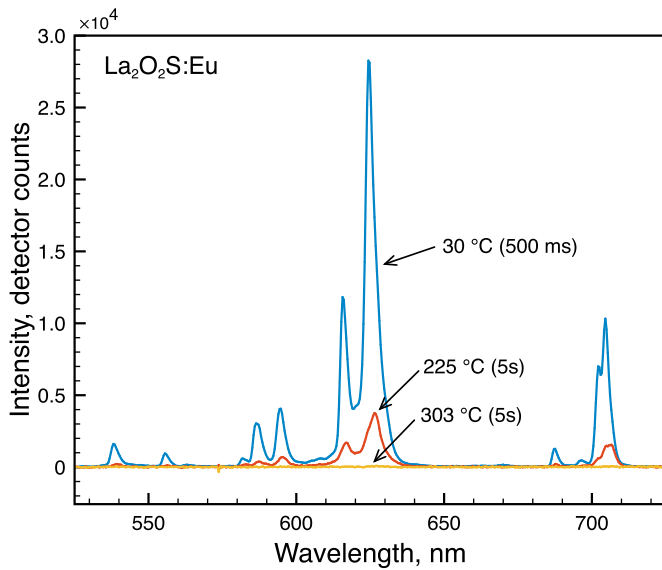
Figure 5. The non-normalized emission spectra of La$_2$O$_2$S:Eu at various temperatures. Note the change in spectrometer integration time at each temperature listed in parentheses in the figure labels.

Figure 6. The non-normalized emission spectra of ZnGa$_2$O$_4$:Mn at two different temperatures. The spectrometer integration time was set to 3 s when capturing these spectra.

shows the emission spectra captured in this study for this phosphor at various temperatures. Emission is observed in the regions predicted from the energy band gaps for Dy^{3+} noted above. Also note a gradual increase in a peak centered near 456 nm with increasing temperature. This is due to pumping of a so-called G level (^{4}I$_{15/2}$) of Dy^{3+} from an F level (^{4}F$_{9/2}$) due to thermalization, which then transitions back to the ground state [34, 35]. The shaded areas in the top plot of figure 4 represent spectral bands of YAG:Dy used in literature to produce temperature-dependent intensity ratio calibrations [35]. These correspond to the regions 467 ± 5 nm and 496 ± 2.5 nm. The bottom plot of figure 4 shows an intensity ratio calibration between these two bands using the present data by ratioing the average intensity of each band at each temperature. This curve indicates how the emission of this phosphor could be used for thermometry when using incident x-rays for excitation.

4.4. La$_2$O$_2$S:Eu

The spectral lines present in the emission spectra of La$_2$O$_2$S:Eu originate from various transitions from the ^{5}D states to the ^{7}F states of Eu^{3+} [32]. The charge transfer state (CTS) of the La$_2$O$_2$S host lattice overlaps the ^{5}D states, creating relaxation pathways between the ^{5}D states. As temperature increases, larger populations are pumped to the higher ^{5}D states. These then follow the CTS to the lower ^{5}D$_J$ states, causing thermal quenching of the emission originating from these states in the order of $J = 3, 2, 1$, and 0 [36–39]. Figure 5 shows the emission spectra collected for this phosphor. As expected, these transitions remain sensitive to temperature when excited by x-ray radiation. Note the changes in integration time set on the spectrometer listed in the labels of this plot. Integration time needed to be increased at higher temperatures to collect more phosphor emission and fully resolve the structure of each spectra. Even so, emission from this phosphor appears to be
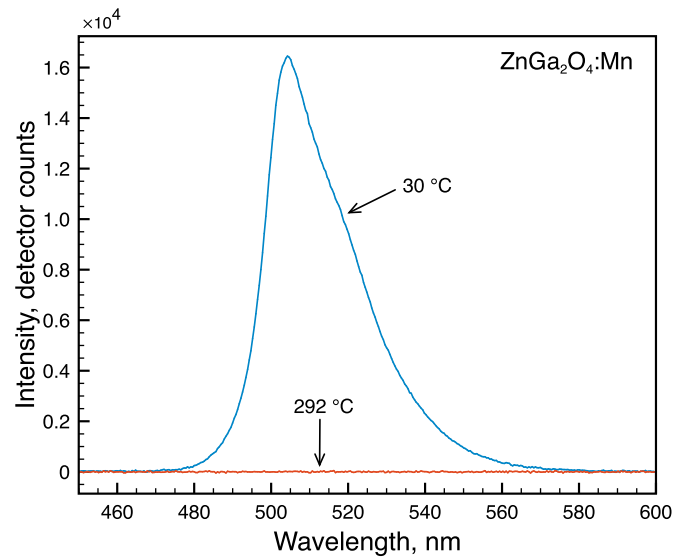
completely thermally quenched above 300 °C. This thermal quenching appears to be more pronounced in the emission of this phosphor under x-ray excitation when compared to UV excitation in a similar temperature range [40].

4.5. ZnGa$_2$O$_4$:Mn

A single broad emission line is typically seen in the emission spectra of ZnGa$_2$O$_4$:Mn centered near 500 nm. This is a consequence of the of the ^{4}T$_1$(^{4}G) → ^{6}A$_1$(^{6}S) transition of Mn^{2+} [32, 41–43]. Figure 6 shows the emission spectra captured from this phosphor during x-ray excitation. Thermal quenching of the emission to background levels is apparent at elevated temperatures near 300 °C. However, no increments of temperature were able to be tested while at the beamline during the present study due to time constraints, therefore further analysis of this phosphor should be performed in the future to fully capture its response to temperature under x-ray excitation.

4.6. Mg$_3$F$_2$GeO$_4$:Mn

The phosphor Mg$_3$F$_2$GeO$_4$:Mn emits in the red region, with spectral bands between 600 and 700 nm [30, 44]. These are a result of the ^{2}E → ^{4}A$_2$ transition of its Mn^{4+} activator [32, 45]. The emission spectra from this phosphor under x-ray excitation are shown in figure 7. The spectral lines observed are in the expected positions, however, like Y$_2$SiO$_5$:Ce, low phosphor intensity is observed. An offset is observed in the average emission spectra at 190 °C due to the proximity of all spectral bands to background noise. This further indicates that emission from this phosphor did not rise above background levels. It can be concluded that it would be difficult to resolve emission from this phosphor in practical applications, limiting its potential for thermometry measurements with x-ray excitation. Even so, these emission spectra do
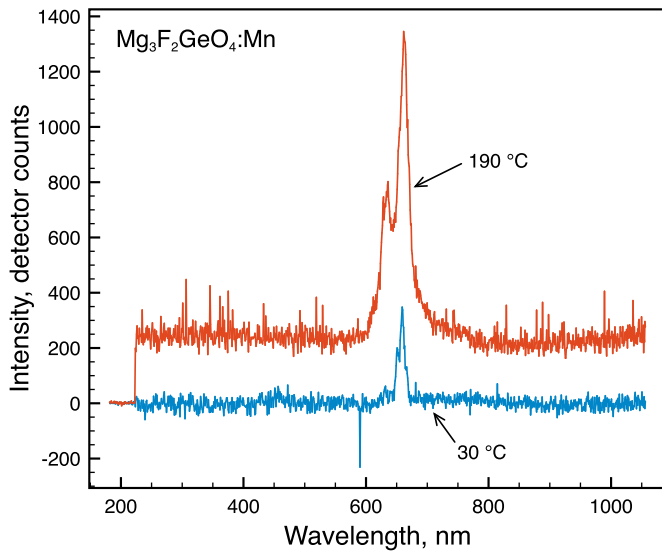
Figure 7. The non-normalized emission spectra of $Mg_3F_2GeO_4$:Mn at two different temperatures. The spectrometer integration time was set to 5 s when capturing these spectra.

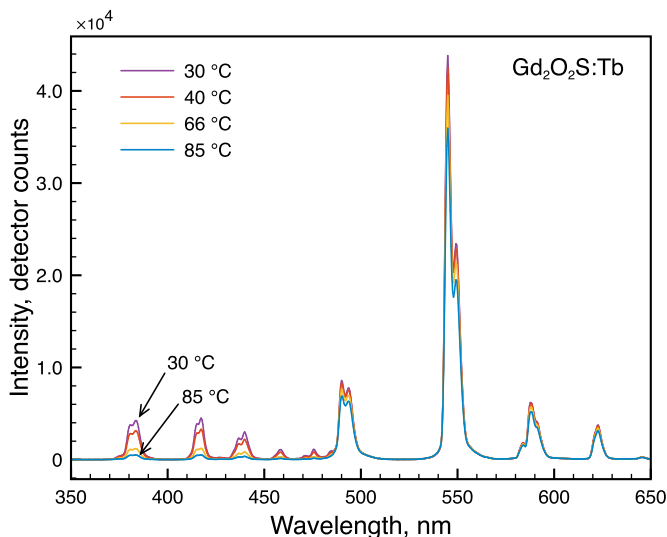**Figure 8.** The non-normalized emission spectra of Gd_2O_2S:Tb at various temperatures. The spectrometer integration time was set to 250 ms when capturing these spectra.

Figure 9. Select peaks in the emission spectra of Gd_2O_2S:Tb captured in the present study at the Advanced Photon Source (top) and using an x-ray tube source located at Sandia National Laboratories (bottom) [17]. Note the spectra shown here are not normalized.

appear to indicate that more thermal quenching occurs with this phosphor under x-ray excitation compared to visible excitation [40].

4.7. Gd_2O_2S:Tb

Many distinct spectral lines are present in the emission spectra of Gd_2O_2S:Tb. These result from several $^5D \rightarrow {^7F}$ transitions of the Tb^{3+} ions doped into this phosphor [32, 46]. While commonly used as an x-ray scintillator, this phosphor has also been used for thermography utilizing a UV excitation source [28, 47]. Temperature sensitivity in these previous studies was shown to be in the range of about 25 °C–100 °C, so this range was used in the current study. Figure 8 shows the spectra
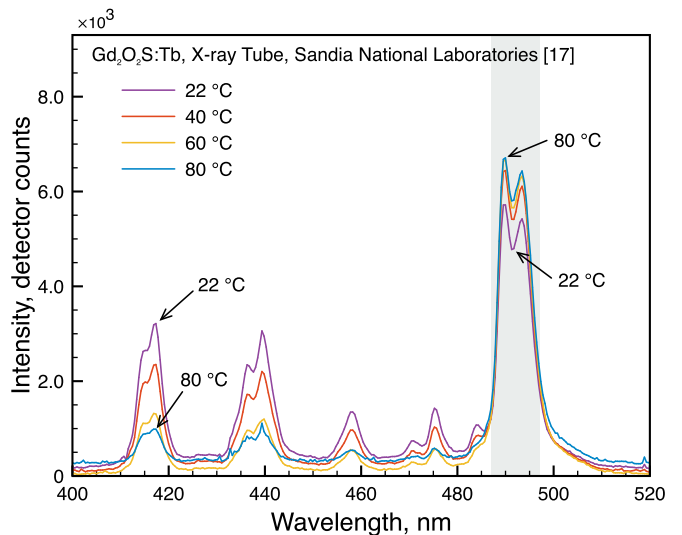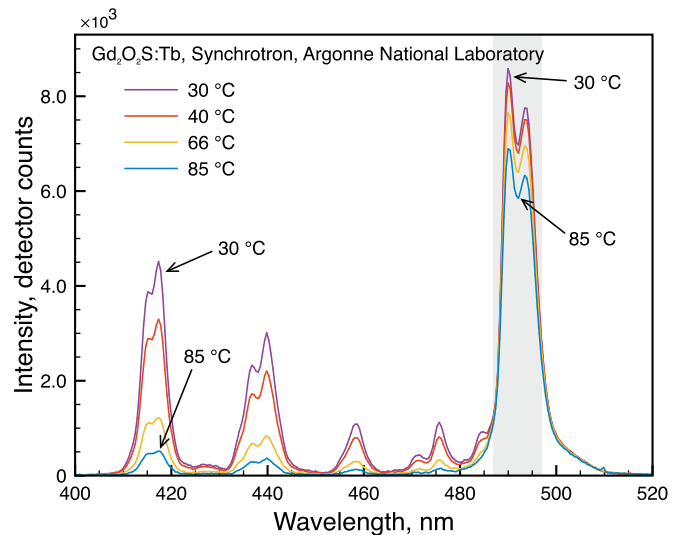
gathered in this range at the Advanced Photon Source. Like the other phosphors reported here, attenuation of emission intensity is observed here in all spectral lines of Gd_2O_2S:Tb.

A previous study from our group focused on the spectral response to temperature of Gd_2O_2S:Tb, instead using a tube x-ray source for excitation of a premade phosphor screen containing this phosphor [17]. Similar attenuation was observed in the response of this phosphor during excitation from the x-ray tube in all but one of its spectral lines. This anomalous spectral line, centered near 490 nm, was observed to increase in intensity with increasing temperature. Figure 9 shows the response of select spectral lines from the present study and our previous study. The shaded region in each plot highlights the spectral line currently being considered centered near 490 nm. This line corresponds to the $^5D_4 \rightarrow {^7F_6}$ transition of Tb^{3+} [46]. The top plot shows the spectra from the current study in which this line in the shaded region is seen to attenuate with increasing
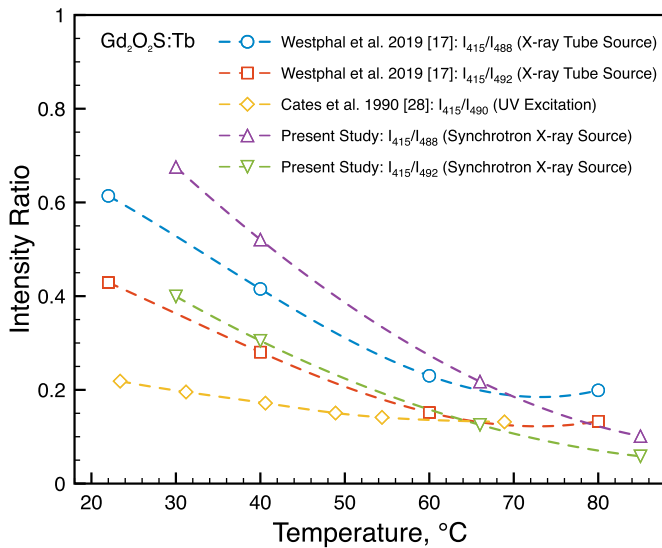
Figure 10. Several intensity ratio curves calculated from select bands in the emission spectra of Gd_2O_2S:Tb from the present study and compared to those found in literature [17, 28]. The spectral bands used in the ratio and the excitation source are listed in the plot legend.

temperature. However, in the bottom plot showing the spectra from our previous study [17], an opposite trend is seen in this region. The unusual behavior from this single peak is most likely due to interference from the coating applied to the premade phosphor screen used in our previous study, though future work should confirm whether this explanation is sufficient by characterizing the emission of samples prepared with Gd_2O_2S:Tb powder and excited by this x-ray tube.

Nevertheless, intensity ratio calibration curves were calculated in our previous study using this spectral line centered near 490 nm along with the line centered near 415 nm [17]. An identical calculation was performed using data collected in the present study, and all temperature calibration curves are plotted together in figure 10. Each intensity ratio used the average intensity of the 415 nm band in the numerator. The average of two different spectral bands were used in the denominator, one centered at 488 nm and another centered at 492 nm. All spectral bands were set to have a width of 10 nm. These spectral regions were selected based upon commercially available optical bandpass filters from Edmund Optics. Also plotted here is a calibration curve found by Cates *et al.* in which this phosphor was excited using a UV lamp [28]. Note the slight difference in center wavelengths of the spectral bands used in the ratio calculated by Cates *et al.* found in the legend of figure 10. All curves exhibit good sensitivity to temperature, with increased sensitivity seen from the phosphors excited by an x-ray source compared to the UV source with the selected spectral bands for ratio calculation.

5. Conclusions

The spectral response of several phosphors induced by incident x-rays was characterized in this study at various temperatures. The general trend observed was attenuation of spectral line intensities with increasing temperature, which is to be expected due to the increased probabilities of non-radiative energy transfer these phosphors experience at elevated temperatures.

The induced emission of all the phosphors reported here show good sensitivity to temperature, which indicates their potential usefulness for thermometry measurements using incident x-rays for excitation. The only exceptions are Y_2SiO_5:Ce and $Mg_3F_2GeO_4$:Mn, whose emission spectra did not rise substantially above background noise levels, and ZnO. This latter phosphor was tested in a similar manner to the other phosphors in this study, although no emission spectra are reported here as none were observed at any of the temperatures tested. One possible reason for this is the thermal promotion of all populations to vibrational levels in the excited electronic state above an intersection point between the excited and ground electronic states of the phosphors, causing these populations to relax back down to the ground state non-radiatively, which may be possible with high energy incident radiation [22]. This could also explain the relatively rapid thermal quenching observed in the emission of Y_2SiO_5:Ce, La_2O_2S:Eu, and $ZnGa_2O_4$:Mn in this study.

Of the phosphors tested, BAM, YAG:Dy, and Gd_2O_2S:Tb show the most promise for phosphor thermometry measurements at elevated temperatures during x-ray excitation. These three showed shifts in spectral properties in the temperature ranges tested here without quenching thermally, indicating that their sensitivity to temperature could extend beyond those tested here. Therefore, future work should focus on fully characterizing the emission of these phosphors induced by x-rays by extending the maximum temperatures beyond the roughly 300 °C limit here. In addition, finer temperature increments should be performed when studying all the phosphors considered in the present study to fully capture their response to temperature. Nevertheless, these results indicate that the response from several thermographic phosphors remains sensitive to temperature when excited via x-rays. This suggests that future measurement techniques can take advantage of this phenomenon to measure surface temperature where incident x-rays are already in place or as a replacement for the typical laser source in certain applications.

Data availability statement

The data that support the findings of this study are available upon reasonable request from the authors.

Acknowledgments

ORCID iDs

Eric R Westphal ⦿ https://orcid.org/0000-0003-3405-3760
Alan L Kastengren ⦿ https://orcid.org/0000-0003-0253-6258
Steven F Son ⦿ https://orcid.org/0000-0001-7498-2922
Terrence R Meyer ⦿ https://orcid.org/0000-0002-2071-142X
Kathryn N G Hoffmeister ⦿ https://orcid.org/0000-0002-0335-9137

References

[1] Casey A D, Roberts Z A, Satija A, Lucht R P, Meyer T R and Son S F 2019 Dynamic imaging of the temperature field within an energetic composite using phosphor thermography *Appl. Opt.* **58** 4320–5

[2] Sabadell A J, Wenograd J and Summerfield M 1965 Measurement of temperature profiles through solid-propellant flames using fine thermocouples *AIAA J.* **3** 1580–4

[3] Parr T P and Hanson-Parr D M 1996 Solid propellant diffusion flame structure *Symp. Combustion* vol 26 pp 1981–7

[4] Heitor M V and Moreira A L N 1993 Thermocouples and sample probes for combustion studies *Prog. Energy Combust. Sci.* **19** 259–78

[5] Bradley D and Matthews K J 1968 Measurement of high gas temperatures with fine wire thermocouples *J. Mech. Eng. Sci.* **10** 299–305

[6] Levendis Y A, Estrada K R and Hottel H C 1992 Development of multicolor pyrometers to monitor the transient response of burning carbonaceous particles *Rev. Sci. Instrum.* **63** 3608–22

[7] Aldén M, Omrane A, Richter M and Särner G 2011 Thermographic phosphors for thermometry: a survey of combustion applications *Prog. Energy Combust. Sci.* **37** 422–61

[8] Brübach J, Pflitsch C, Dreizler A and Atakan B 2013 On surface temperature measurements with thermographic phosphors: a review *Prog. Energy Combust. Sci.* **39** 37–60

[9] Särner G, Richter M and Aldén M 2008 Investigations of blue emitting phosphors for thermometry *Meas. Sci. Technol.* **19** 125304

[10] Heyes A L, Seefeldt S and Feist J P 2006 Two-colour phosphor thermometry for surface temperature measurement *Opt. Laser Technol.* **38** 257–65

[11] Omrane A, Ossler F and Aldén M 2002 Two-dimensional surface temperature measurements of burning materials *Proc. Combust. Inst.* **29** 2653–9

[12] Khalid A H and Kontis K 2009 2D surface thermal imaging using rise-time analysis from laser-induced luminescence phosphor thermometry *Meas. Sci. Technol.* **20** 025305

[13] Allison S W, Beshears D L, Cates M R, Paranthaman M and Gilles G T 2001 LED-induced fluorescence diagnostics for turbine and combustion engine thermometry *Opt. Diagnostics Fluids, Solids, Combust.* vol 4448 pp 28–35

[14] Allison S W, Cates M R and Gillies G T 2002 Excitation of thermographic phosphors using a blue light emitting diode: spectral characteristics and instrumentation applications *Rev. Sci. Instrum.* **73** 1832

[15] Atakan B, Eckert C and Pflitsch C 2009 Light emitting diode excitation of $Cr^{3+}:Al_2O_3$ as thermographic phosphor: experiments and measurement strategy *Meas. Sci. Technol.* **20** 075304

[16] Flores-Brito W, Westphal E, Wilburn B R and Gabet Hoffmeister K N 2019 Study of sensitivity vs. excitation time of LED excited thermographic phosphors *AIAA Scitech 2019 Forum* (https://doi.org/10.2514/6.2019-2106)

[17] Westphal E R, Son S F, Quintana E and Hoffmeister K N G 2019 X-ray excitation of thermographic phosphors *11th US National Combustion Meeting*

[18] Allison S W, Baker E S, Lynch K J and Sabri F 2017 *In vivo* x-ray excited optical luminescence from phosphor-doped aerogel and Sylgard 184 composites *Radiat. Phys. Chem.* **135** 88–93

[19] Chen H, Longfield D E, Varahagiri V S, Nguyen K T, Patrick A L, Qian H, Vanderveer D G and Anker J N 2011 Optical imaging in tissue with x-ray excited luminescent sensors *Analyst* **136** 3438–45

[20] Rodnyi P A 1997 *Physical Processes in Inorganic Scintillators* vol 14 (Boca Raton, FL: CRC Press)

[21] Birks J B 1964 The scintillation process in inorganic crystals—I *The Theory and Practice of Scintillation Counting* (Oxford: Pergamon Press) pp 68–95

[22] Khalid A H and Kontis K 2008 Thermographic phosphors for high temperature measurements: principles, current state of the art and recent applications *Sensors* **8** 5673–744

[23] Brübach J, Janicka J and Dreizler A 2009 An algorithm for the characterisation of multi-exponential decay curves *Opt. Lasers Eng.* **47** 75–79

[24] Feist J P, Heyes A L, Choy K L and Su B 1999 Phosphor thermometry for high temperature gas turbine applications *ICIASF 99. 18th Int. Congr. Instrum. Aerosp. Simul. Facil. Rec. (Cat. No.99CH37025) 6/1-6/7* (https://doi.org/10.1109/ICIASF.1999.827145)

[25] Allison S W and Gillies G T 1997 Remote thermometry with thermographic phosphors: instrumentation and applications *Rev. Sci. Instrum.* **68** 2615

[26] Nikl M 2006 Scintillation detectors for x-rays *Meas. Sci. Technol.* **17** R37–54

[27] Issler S L and Torardi C C 1995 Solid state chemistry and luminescence of x-ray phosphors *J. Alloys Compd.* **229** 54–65

[28] Cates M R, Tobin K W and Barton Smith D 1990 *Evaluation of Thermographic Phosphor Technology for Aerodynamic Model Testing* (Oak Ridge, TN: Oak Ridge National Lab., Applied Technology Div.) (https://doi.org/10.2172/6318237)

[29] Abram C, Fond B and Beyrau F 2015 High-precision flow temperature imaging using ZnO thermographic phosphor tracer particles *Opt. Express* **23** 19453–68

[30] Nada F A, Knappe C, Xu X, Richter M and Aldén M 2014 On the automation of thermographic phosphor calibration *IET ISA 60th Int. Instrum. Symp. 2014* (https://doi.org/10.1049/cp.2014.0548)

[31] Yan Y, Zhang X, Li H, Ma Y, Xie T, Qin Z, Liu S, Sun W and Lewis E 2018 An optical fiber sensor based on La$_2$O$_2$S:Eu scintillator for detecting ultraviolet radiation in real-time *Sensors* **18** 3754

[32] Shionoya S, Yen W M and Yamamoto H 1997 *Phosphor Handbook* (Boca Raton, FL: CRC Press)

[33] Nau P, Yin Z, Geigle K P and Meier W 2017 Wall temperature measurements at elevated pressures and high temperatures in sooting flames in a gas turbine model combustor *Appl. Phys.* B **123** 279

[34] Kontis K, Syogenji Y and Yoshikawa N 2002 Surface thermometry by laser-induced fluorescence of Dy^{3+}:YAG *Aeronaut. J.* **106** 453–7

[35] Goss L P, Smith A A and Post M E 1989 Surface thermometry by laser-induced fluorescence *Rev. Sci. Instrum.* **60** 3702–6

[36] Fonger W H and Struck C W 1970 Eu^{+3} ^{5}D resonance quenching to the charge-transfer states in Y$_2$O$_2$S, La$_2$O$_2$S, and LaOCl *J. Chem. Phys.* **52** 6364–72

[37] Struck C W and Fonger W H 1970 Role of the charge-transfer states in feeding and thermally emptying the ^{5}D states of Eu^{+3} in yttrium and lanthanum oxysulfides *J. Lumin.* **1–2** 456–69

[38] Yap S V, Ranson R M, Cranton W M and Koutsogeorgis D 2008 Decay time characteristics of La$_2$O$_2$S:Eu and La$_2$O$_2$S:Tb for use within an optical sensor for human skin temperature measurement *Appl. Opt.* **47** 4895–9

[39] Krauss R H, Hellier R G and McDaniel J C 1994 Surface temperature imaging below 300 K using La$_2$O$_2$S:Eu *Appl. Opt.* **33** 3901–4

[40] Bugos A R 1989 Characterization of the emission properties of thermographic phosphors for use in high temperature sensing application (Knoxville, TN: University of Tennessee)

[41] Brübach J, Kissel T, Frotscher M, Euler M, Albert B and Dreizler A 2011 A survey of phosphors novel for thermography *J. Lumin.* **131** 559–64

[42] Minami T, Maeno T, Kuroi Y and Takata S 1995 High-luminance green-emitting thin-film electroluminescent devices using ZnGa$_2$O$_4$:Mn phosphor *Japan. J. Appl. Phys.* **34** L684–7

[43] Minami T, Miyata T, Takata S and Fukuda I 1991 High-luminance green Zn$_2$SiO$_4$:Mn thin-film electroluminescent devices using an insulating BaTiO$_3$ ceramic sheet *Japan. J. Appl. Phys.* **30** L117–9

[44] Nada F A, Knappe C, Xu X, Richter M and Aldén M 2014 Development of an automatic routine for calibration of thermographic phosphors *Meas. Sci. Technol.* **25** 025201

[45] Knappe C 2013 Phosphor thermometry on surfaces—A study of its methodology and its practical applications *PhD Thesis* Lund University

[46] Popovici E J, Muresan L, Hristea-Simoc A, Indrea E, Vasilescu M, Nazarov M and Jeon D Y 2004 Synthesis and characterisation of rare earth oxysulphide phosphors. I. Studies on the preparation of Gd$_2$O$_2$S:Tb phosphor by the flux method *Opt. Mater.* **27** 559–65

[47] Allison S, Cates M and Beshears D 2000 A survey of thermally sensitive phosphors for pressure sensitive paint applications *Proc. Int. Instrumentation Symp.* vol 46 pp 29–38